Gulf Journal of Mathematics ISSN: 2309-4966
Vol 19, Issue 2 (2025) 369-383 https://doi.org/10.56947/gjom.v19i2.2765

NONLINEAR DYNAMICS AND CHAOS IN FRACTIONAL-ORDER CARDIAC ACTION POTENTIAL DURATION MAPPING MODEL WITH FIXED MEMORY LENGTH

AIDA BELLOUT[1,2], RABAH BOUOUDEN[1,2], TAREK HOUMOR[3] and MESSAOUD BERKAL[2,4,*]

Abstract. In this paper, a novel one-dimensional mapping model for cardiac action potential duration (APD) is proposed, introducing the concept of "fixed memory length" within a fractional-order discrete framework. Unlike traditional fractional models with infinite memory or short-memory maps, this approach explicitly incorporates a controlled memory span, allowing a more realistic representation of cardiac tissue dynamics. The model reveals new nonlinear behaviors influenced by memory effects, analyzed through bifurcation diagrams and validated using the $0-1$ test for chaos under varying pacing periods (t_s). The results demonstrate that fixed memory length plays a fundamental role in dynamic instability, leading to alternans and chaotic behaviors. Clinically, this modeling provides deeper insight into the mechanisms underlying cardiac arrhythmias and irregular rhythms, offering potential applications to improve arrhythmia prediction and guide therapeutic pacing strategies.

1. Introduction

Chaos theory is a captivating field of mathematics that delves into the behavior of dynamic systems that are highly sensitive to initial conditions, a phenomenon famously known as the "butterfly effect." Although its roots lie in meteorology and classical mechanics, chaos theory has expanded its influence across disciplines such as biology, economics, engineering, and social sciences [2, 3, 4, 5, 6, 7, 8, 16, 18, 20, 25, 26, 35]. Contrary to popular belief, chaos does not imply randomness; rather, it describes deterministic systems whose complexity renders their outcomes highly unpredictable [29].

The applications of chaos theory are diverse and impactful: in medicine, it aids in modeling irregular heart rhythms; in ecology, it explains population dynamics; and in finance, it provides insights into market volatility [38]. Furthermore, chaos theory has driven innovations in secure communication systems and algorithm optimization [9, 10, 11]. By uncovering the intricate patterns underlying seemingly

Date: Received: Mar 12, 2025; Accepted: Mar 31, 2025
* Corresponding author.
2020 *Mathematics Subject Classification.* Primary 39A33, 37N30; Secondary 37D45.
Key words and phrases. Cardiac action potential duration, fixed memory length, bifurcation, chaos.

erratic behaviors, chaos theory challenges traditional notions of order and provides tools for predicting and managing complex phenomena in an ever-changing world [19].

In cardiology, chaos theory has proven invaluable for understanding the dynamics of cardiac action potential duration (APD) and its restitution properties. Low-dimensional iterated maps have been particularly effective in modeling the relationship between APD and the preceding diastolic interval. These models offer critical insights into the onset of irregular rhythms, such as alternans and arrhythmias, by linking the stability of heart rhythms to the slope of the APD restitution curve. When this slope exceeds a critical threshold, instabilities such as APD alternans can arise, potentially leading to life-threatening fibrillation. Extensive experimental validation highlights the utility of these models in both healthy and diseased hearts, and they have guided the development of therapeutic strategies like pacing algorithms to mitigate arrhythmias [24, 32, 36, 41].

Short memory in APD models assumes that the current action potential duration is influenced only by a limited number of preceding cardiac cycles, allowing the dynamics to focus primarily on recent states. These low-dimensional iterated maps have proven effective in capturing essential features of cardiac rhythm, particularly under specific conditions where the influence of earlier cycles is minimal. However, such traditional short-memory or memoryless models often fail to represent the long-range dependencies and cumulative effects inherently present in biological systems, especially in the complex dynamics of cardiac APD. In reality, cardiac tissue exhibits memory-like behavior, where ionic concentrations, channel states, and previous excitations influence future responses over extended time scales. Neglecting these cumulative effects restricts the model's ability to predict intricate arrhythmogenic behaviors, including the emergence of alternans, complex periodicities, and chaotic dynamics. Therefore, when longer memory effects become significant, higher-dimensional or fractional dynamic systems become necessary to accurately account for the influence of more distant past cycles on present dynamics [17, 27, 30, 33, 34, 39].

Fractional-order models with fixed-length memory have emerged as a powerful alternative to overcome these limitations. By explicitly incorporating a defined memory span, these models extend beyond recent cycles and integrate both short- and long-term historical influences on the current APD. This not only enhances the model's capacity to reproduce nonlinear phenomena such as bifurcations and chaos but also provides deeper insights into the memory-driven mechanisms that underlie cardiac alternans and arrhythmias. Such an approach delivers a more physiologically realistic framework, improving the predictive power of computational models and potentially guiding more effective therapeutic strategies for managing cardiac rhythm disorders. In [23], Guel-Cortez and Kim explore the application of fractional-order derivatives in cardiovascular system modeling, demonstrating their effectiveness in replicating various cardiac anomalies, such as aortic regurgitation and ischemic cardiomyopathy. Stenzinger and Tragtenberg [37] employ map-based models to simulate complex cardiac dynamics, successfully reproducing arrhythmic behaviors like torsade de pointes with fewer parameters than traditional conductance-based models.

Recent studies have increasingly emphasized the critical role of memory effects and fractional-order dynamics in cardiac electrophysiological modeling. For instance, Wang et al. [40] demonstrated that intracellular ionic accumulation significantly alters APD dynamics under pathological conditions, leading to complex nonlinear behaviors and memory-induced chaos in cardiac tissue. Similarly, Zhao et al. [43] advanced space-fractional cardiac models, showing improved accuracy in simulating wave propagation by incorporating non-local interactions and memory effects. However, most existing models either assume infinite memory kernels or do not explicitly explore the impact of memory on nonlinear bifurcation and chaotic behavior. Building upon this emerging research, our study introduces a novel discrete fractional-order APD mapping model with fixed memory length. This allows systematic investigation of how memory truncation influences dynamic instability, alternans, and chaos. By offering a controllable memory horizon, our model bridges the gap between idealized long-memory formulations and physiologically constrained memory effects, providing new insights into arrhythmogenesis mechanisms and enhancing cardiac rhythm modeling frameworks.

This study aims to investigate the nonlinear dynamics of a discrete fractional-order mapping model for cardiac action potential duration (APD) that explicitly incorporates fixed-length memory effects. Building upon the classical one-dimensional mapping model (1D-map) introduced by Lewis and Guevara [28], the proposed model extends its capability by integrating memory-driven influences to capture more complex dynamical behaviors. To thoroughly analyze the system's response under varying conditions, bifurcation diagrams are constructed to visualize transitions in rhythmic patterns and identify the onset of dynamic instabilities. Additionally, the $0-1$ test for chaos is applied to rigorously distinguish between regular and chaotic regimes, offering deeper insights into the model's potential to replicate arrhythmogenic phenomena observed in cardiac tissues.

2. Necessary Definitions in Discrete Fractional Calculus

This section focuses on exploring essential definitions from discrete fractional calculus.
Let $b \in \mathbb{R}$ and let $\mathbb{N}_b = \{b, b+1, b+2, ...\}$ denotes the discrete time scale. For the function $u(n)$, the delta difference operator Δ is given by

$$\Delta u(n) = u(n+1) - u(n). \tag{2.1}$$

Definition 2.1 ([31])**.** Let $u : \mathbb{N}_b \longrightarrow \mathbb{R}$ and $v > 0$. Then the fractional sum of v order is expressed as

$$\Delta_b^{-v} u(t) = \frac{1}{\Gamma(v)} \sum_{r=b}^{t-v} (t - \delta(r))^{(v-1)}\, u(r),\ t \in \mathbb{N}_{b+v}, \tag{2.2}$$

where b represents the initial point, $\delta(r) = r + 1$ and $t^{(v)}$ is the falling function defined in terms of the Gamma function as

$$t^{(v)} = \frac{\Gamma(t+1)}{\Gamma(t+1-v)}. \tag{2.3}$$

Definition 2.2 ([1])**.** For $v > 0$, $v \notin \mathbb{N}$ and $u(t)$ defined on $\mathbb{N}_b$, the Caputo-like delta difference is defined by

$$
\begin{aligned}
{}^c\Delta_b^v u(t) &= \Delta_b^{-(m-v)} \Delta^m u(t), && (2.4)\\
&= \frac{1}{\Gamma(m-v)} \sum_{r=b}^{t-(m-v)} (t-\delta(r))^{(m-v-1)} \Delta_r^m u(r), && (2.5)
\end{aligned}
$$

where $t \in \mathbb{N}_{b+m-v}$, $m = [v] + 1$.

Theorem 2.3 ([14])**.** *For the delta fractional difference equation*

$$
\begin{cases}
{}^c\Delta_b^v u(t) = g(t+v-1, u(t+v-1)),\\
\Delta^k u(b) = u_k, \quad m = [v]+1, \quad k = 0, \ldots, m-1.
\end{cases}
$$

The equivalent discrete integral equation can be formulated as

$$
u(t) = u_0(t) + \frac{1}{\Gamma(v)} \sum_{r=b+m-v}^{t-v} (t-\delta(r))^{(v-1)} \times g(r+v-1, u(r+v-1)), \; t \in \mathbb{N}_{b+m}, \tag{2.6}
$$

where

$$
u_0(t) = \sum_{k=0}^{m-1} \frac{(t-b)^{(b)}}{k!} \Delta^k u(b). \tag{2.7}
$$

The Caputo-like delta difference is a discrete fractional operator that generalizes the traditional difference operation to account for memory effects. Unlike the standard difference, which considers only the immediate previous state, the fractional delta difference allows the current state to depend on a weighted sum of all past states, with weights decreasing over time. This property effectively captures the fading memory behavior observed in complex systems, especially biological ones. The key motivation for using the Caputo-like form is its suitability for modeling systems where the influence of the past fades gradually rather than abruptly-just like in cardiac tissue, where previous action potentials affect current behavior but with diminishing strength over time. Such behavior is well-represented by fractional-order models, which inherently encode memory and hereditary properties [1, 14]. Mathematically, the Caputo-like definition ensures that initial conditions can be applied in a way similar to classical models, making it more intuitive and practical for physical and biological systems, particularly in bioengineering applications where physiological systems naturally exhibit memory effects [30].

3. One Dimensional fractional cardiac action potential duration map with fixed memory length

The cardiac system is an excitable dynamic system with memory properties, but understanding how this memory affects the excitation dynamics remains a challenge. Numerical simulations conducted in [27] on APD models showed that memory plays a fundamental role in dynamic instability, leading to complex and chaotic excitation behaviors. The effect of memory on cardiac alternans has received attention from many previous studies, including [15, 17, 33, 34]. These studies found that memory can either suppress cardiac alternans or enhance dynamic instability, resulting in chaotic behaviors in APD cardiac models. This phenomenon is accurately represented by a recurrent mapping model that takes memory effects into account. To determine the effect of fixed-length memory on the dynamics of the model, a one-dimensional mapping that does not include memory is first analyzed. This special class of APD maps, proposed in [28], is a fundamental model for understanding cardiac dynamics.

The Lewis and Guevara model is a widely used mathematical framework for describing excitable cardiac cells, particularly in the study of cardiac arrhythmias. However, traditional formulations typically rely on integer-order differential equations, which assume instantaneous interactions and complete memory loss beyond a specific time frame. This simplification may not fully capture the intricate biophysical processes underlying cardiac dynamics. Extending the Lewis and Guevara model using fractional calculus and fixed-length memory introduces key physiological and physical refinements. The mathematical definition is given by:

$$x(i+1) = g(x(i)),\ i \in \mathbb{N},$$

or

$$x(i+1) = A - B_1 \exp\left(\frac{x(i)-nt_s}{\tau_1}\right) - B_2 \exp\left(\frac{x(i)-nt_s}{\tau_2}\right), \tag{3.1}$$

$x(i) \in [0, 270msec]$, where $x(i+1)$ is the APD generated by the $(i+1)$th stimulus and let n the parameter block in the production of an action potential on the condition that $(nt_s - x(i+1) \geq DI_{\min})$. The constants $A, B_1, B_2, \tau_1, \tau_2, DI_{\min}$ are related to the cardiac electrophysiological constraints of the heart, as defined by Lewis and Guevara [28]. These parameters are as follows:

$$A = 270msec,\ B_1 = 2441msec,\ B_2 = 90.02msec,$$

$$\tau_1 = 19.6msec,\ \tau_2 = 200.5msec,\ DI_{\min} = 53.5msec.$$

These parameters are derived from well-established cardiac electrophysiological constraints, based on experimental data on ion channel kinetics, action potential durations, and refractory periods in cardiac tissues. The chosen values ensure the biological plausibility of the model and are consistent with observed electrophysiological behaviors in real cardiac cells.

Figure 1 shows a bifurcation diagram inspired by the study of Lewis and Guevara [28], where cardiac tissue has a stable natural rhythm of 1 : 1 at long pacing intervals, meaning that each stimulus produces an action potential of equal duration. As heart rate accelerates (i.e., the pacing interval decreases), this rhythm loses its stability, resulting in alternating rhythmic patterns, such as the 2 : 2 rhythm. In this study, the dynamic relationship between the pacing interval, the action potential time (APD), and the diastolic interval (DI) is described by the equation: $DI(i+1) = nt_s - x(i)$, where t_s denotes the basic pacing interval. As the frequency of the stimulus increases, Figure 1 defines the bifurcation sequence

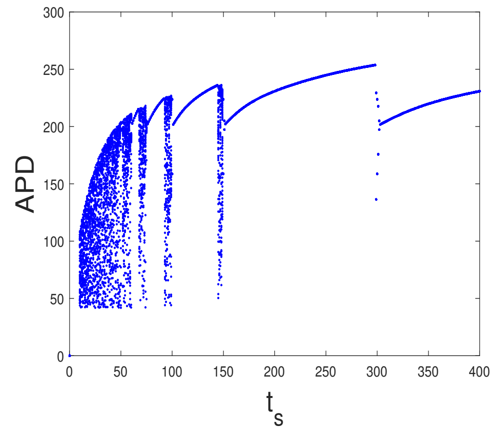

FIGURE 1. The bifurcation diagram reveals the presence of alternans rhythm, bistability, and a period-doubling bifurcation pathway leading to chaos in the map (3.1).

of rhythms for any initial value $x(1) \leq 248msec$:
$sequence = \{1:1 \to 2:2 \to 2:1 \to 4:2 \to chaos \to 3:1 \to 6:2 \to chaos \to 4:1 \to 8:2 \to chaos \to 5:1 \to 10:2 \to 6:1 \to chaostotal\}$.
For the initial value $x(1) > 248msec$, the branching sequence is as follows:
$sequence = \{1:1 \to 2:1 \to 4:2 \to chaos \to 3:1 \to 6:2 \to chaos \to 4:1 \to 8:2 \to chaos \to 5:1 \to 10:2 \to chaos \to 6:1 \to chaostotal\}$.
The two previous sequences show the presence of bistability in model (3.1):

- The bistability between two $1:1$ and $2:1$ rhythms at $301.8msec < t_s \leq 307.3msec$.
- The bistability between two $2:2$ and $2:1$ rhythms at $297.9msec < t_s \leq 301.8msec$.

It was also noted that when the repetitions start from any random initial state within the time interval $[0, 270msec]$, the appearance of chaos occurs only when the rhythm $4:2$ loses its stability.
Now we move from the model of Lewis and Guevara without memory to the model with memory, by presenting the fractional version of the map (3.1).
The first-order difference of (3.1) can be easily formulated as:

$$\triangle x_n = A - B_1 \exp\left(\frac{x_n - nt_s}{\tau_1}\right) - B_2 \exp\left(\frac{x_n - nt_s}{\tau_2}\right) - x_n. \tag{3.2}$$

Using the Caputo-like delta difference with d as the starting point, the fractional-order difference of (3.2) is given by

$$^c\triangle_d^v x(t) = A - B_1 \exp\left(\frac{x(t-1+v) - nt_s}{\tau_1}\right) - B_2 \exp\left(\frac{x(t-1+v) - nt_s}{\tau_2}\right) - x(t-1+v). \tag{3.3}$$

According to Theorem 2.3, we consider the generalized fractional model of the model (3.2), given by

$$x_n = x_0 + \frac{1}{\Gamma(v)} \sum_{j=1}^{n} \frac{\Gamma(n-j+v)}{\Gamma(n-j+1)} \left(a - b_1 \exp\left(\frac{x_{j-1} - nt_s}{\tau_1}\right) - b_2 \exp\left(\frac{x_{j-1} - nt_s}{\tau_2}\right) - x_{j-1} \right), \tag{3.4}$$

where $0 < v \leq 1$, v is the fractional order of discrete dynamical system (3.4). Through the fractional order of discrete dynamical system, we find that system (3.4) is subject to the memory effect because the current state x_n is related to all previous states $(x_0, x_1, x_2, ..., x_{n-1})$.

From this we get the idea whether the change in the length of the memory also has an effect on the dynamics, that is, if a fixed length is set for the memory F such that from the initial state x_0 until the state x_F is calculated starting from all previous states, but starting from the state x_{F+1} to the ultimate state x_n is calculated based on F previous states only.

Based on the map (3.4) our proposal is One Dimensional fractional cardiac action potential duration map with fixed memory length as follow

$$\begin{cases} x_n = x_0 + \frac{1}{\Gamma(v)} \sum\limits_{j=1}^{n} \frac{\Gamma(n-j+v)}{\Gamma(n-j+1)} \left(a - b_1 \exp\left(\frac{x_{j-1} - nt_s}{\tau_1}\right) - b_2 \exp\left(\frac{x_{j-1} - nt_s}{\tau_2}\right) - x_{j-1} \right) & \text{if } n \leq F, \\ x_n = \frac{1}{\Gamma(v)} \sum\limits_{j=n-F}^{n} \frac{\Gamma(n-j+v)}{\Gamma(n-j+1)} \left(a - b_1 \exp\left(\frac{x_{j-1} - nt_s}{\tau_1}\right) - b_2 \exp\left(\frac{x_{j-1} - nt_s}{\tau_2}\right) - x_{j-1} \right) & \text{else}, \end{cases} \tag{3.5}$$

where F represents the length of the memory.

Upon analyzing the bifurcation diagram, we find that when $t_s = 400msec$, the system stabilizes in a period-1 orbit, indicating a stable $1:1$ rhythm. As t_s is reduced, period-1 orbit becomes unstable and is replaced by a stable period-2 orbit corresponding to a $2:2$ rhythm or alternans. This period-2 state emerges from a period-doubling bifurcation at $t_s = 305.7msec$. When we reduce the parameter t_s until the value $304.2msec$ we observe the formation of a period-5 which corresponds to a $5:5$ rhythm and lasts up to $t_s = 303msec$, at which point orbit a period-3 state corresponding to a $3:3$ rhythm appears.

When we reduce the parameter ts until the value $301msec$ mse we observe the formation of a period-1 which corresponds to a $2:1$ rhythm. As t_s decreases further, a period doubling bifurcation occurs at $t_s = 152.5msec$, where the $2:1$ rhythm transitions to a $4:2$ rhythm. Following this, an irregular rhythm emerges when t_s reaches a value of $152.1msec$.

As t_s is progressively reduced from $142msec$ to $40msec$ in $0.1msec$ increments, transitions repeatedly occur in the sequence $\{n:1 \to 2n:2 \to irregular \to n+1:1\}$, with n ranging from 3 to 5.

Consequently, when the initial state is $APD_1 = 260msec$, the system's dynamics can be outlined by the following sequence:

$sequence = \{1:1 \to 2:2 \to 5:5 \to 3:3 \to 2:1 \to 4:2 \to chaos \to 3:1 \to 6:2 \to chaos \to 4:1 \to 8:2 \to chaos \to 5:1 \to 10:2 \to chaostotal\}$.

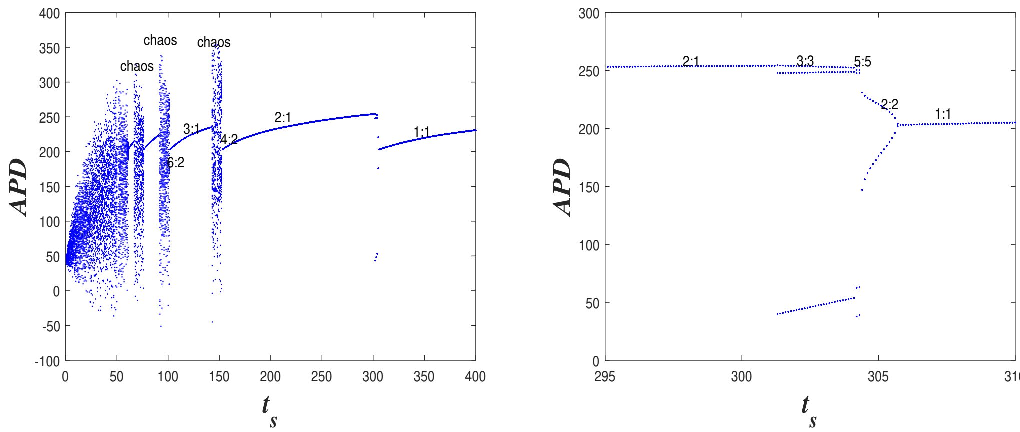

(a) (b)

FIGURE 2. (a) Bifurcation diagram illustrating the presence of alternans rhythm and a period-doubling pathway to chaos in the mapping model (3.5), with a memory length of $F = 2800$, a fractional order of $v = 0.95$, and an initial condition of $APD_1 = 260msec$, (b) Focused view on alternans behavior in the $295msec - 310msec$ range.

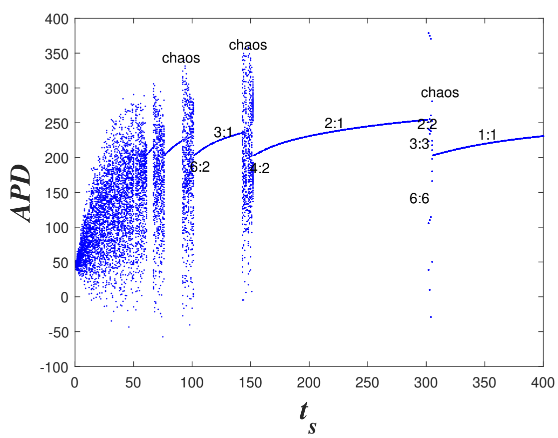

FIGURE 3. Bifurcation diagram for the cardiac mapping model (3.5) (APD vs t_s), illustrating the dynamics of action potential duration with a fixed memory length of $F = 2800$, a fractional order of $v = 0.95$, and an initial condition of $APD_1 = 200msec$.

With an initial condition of $APD_1 = 200msec$, the bifurcation diagram depicted in Figure (3) is obtained. We observe that alternans ($2:2 rhythm$) are absent, and chaos emerges suddenly during a border collision bifurcation. Consequently, we can identify the following sequence of bifurcations:
$sequence = \{1:1 \rightarrow chaos \rightarrow 2:2 \rightarrow 3:3 \rightarrow 6:6 \rightarrow 2:1 \rightarrow 4:2 \rightarrow chaos \rightarrow 3:1 \rightarrow 6:2 \rightarrow chaos \rightarrow 4:1 \rightarrow 8:2 \rightarrow chaos \rightarrow 5:1 \rightarrow 10:2 \rightarrow chaostotal\}$

Bistability is observed in the fractional-order map of APD with a fixed memory length, where iterations converge to one of two orbits based on the selected initial condition,

- Bistability between two $2:2$ and *chaos* rhythms at $304.4msec < t_s \leq 305.7msec$.
- Bistability between two $5:5$ and $3:3$ rhythms at $303msec < t_s \leq 304.2msec$.
- Bistability between two $3:3$ and $6:6$ rhythms at $301msec < t_s \leq 303msec$.

4. Chaos

In this part of the article we use the"$0-1$ test" method, proposed by Gattwald and Melbourne [21] to detect and confirm the presence of chaotic behavior in dynamical systems. The $0-1$ test for chaos is a tool used to distinguish between chaotic and regular behavior in dynamical systems.In our specific modeling context, this test offers several key advantages: as we know many real-world datasets contain measurement noise, which can distort Lyapunov exponent calculations. The 0–1 test is more resilient to noise, ensuring reliable chaos detection even in imperfect data conditions. Also, the test yields a single metric, K, where values close to 1 indicate chaos and values near 0 indicate regular motion. This simplicity facilitates clear decision-making in our modeling framework, avoiding the subjectivity involved in phase-space analysis.
The nature of the system can be determined by dynamics of translation variables p and q, which are defined by the following equations:

$$p_s(n) = \sum_{j=1}^{n} x(j)\cos(js), \tag{4.1}$$

and

$$q_s(n) = \sum_{j=1}^{n} x(j)\sin(js), \tag{4.2}$$

where $s \in [0, \pi]$ is a constant value, and $n = 1, 2, \ldots, N$.
According to the 0-1 test, if the trajectories p and q are bounded, it indicates that the system is not chaotic, while if the p and q are Brownian, then it means that the behavior is chaotic.
The mean square displacement $M_s(n)$ is defined using the following relatioship:

$$M_s(n) = \frac{1}{N}\sum_{j=1}^{N}(p_s(j+n) - p_s(j))^2 + (q_s(j+n) - q_s(j))^2. \tag{4.3}$$

Finally, we determine the asymptotic growth rate K using the correlation method as follows

$$K = \text{median}(k_s), \tag{4.4}$$

where k_s is defined by :

$$k_s = \frac{\mathrm{cov}(\xi, \Delta)}{\sqrt{\mathrm{var}(\xi)\mathrm{var}(\Delta)}} \in [-1, 1], \tag{4.5}$$

$\xi = (1, 2, \cdots, n_{cut}), \Delta = (M_n(1), M_n(2), \cdots, M_n(cut))$ and $n_{cut} = \mathrm{round}(N/10))$, K represents the median of the given k_s values, and covariance and variance of vectors of length $\bar{n}$ are defined as follows:

$$\mathrm{cov}(w, z) = \frac{1}{\bar{n}} \sum_{j=1}^{\bar{n}} (w(j) - \bar{w})(z(j) - \bar{z}),$$

$$\bar{w} = \frac{1}{\bar{n}} \sum_{j=1}^{\bar{n}} w(j), \quad \text{and} \quad \mathrm{var}(w) = cov(w, w).$$

The dynamic behavior of the system can also be determined using the asymptotic growth rate K. If K is close to one, we say that the system evolves chaotically; if K is close to zero, we say that the system dynamic behaves regularly.

Figure 4 represents $0-1$ test results for map (3.5) for fixed memory length of

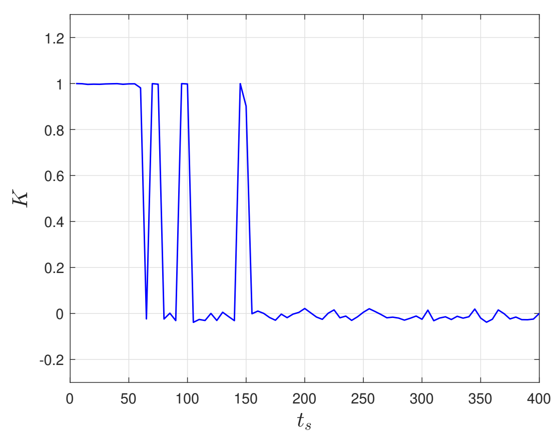

FIGURE 4. Representation of 0-1 test for map (3.5) with fixed memory length $F = 2800$, fractional order $v = 0.95$ and initial condition $APD_1 = 260msec$.

$F = 2800$, fractional order $v = 0.95$ and initial condition $APD_1 = 260msec$. We can see through this shape that when the t_s value is confined between $400msec$ and $155msec$ the K value is close to zero and this indicates the regular behavior of this map (see figure 5 (a)). While when the value of t_s drops from $155msec$ to $140msec$ the value of K rises to one which indicates the chaotic behaviour of this map (see figure 5 (b)). Then we notice the return of the K value to zero when t_s is between $140msec$ to $106msec$. The convergence of K to one is observed again when t_s is between $106msec$ to $90msec$, then the value of K goes to zero when t_s is between $90msec$ and $80msec$, and with the continuous decrease of t_s from $80msec$ to $66msec$, the value of K rises again to near one. However, when $t_s = 65msec$, we notice that the value of K is close to zero,and with further

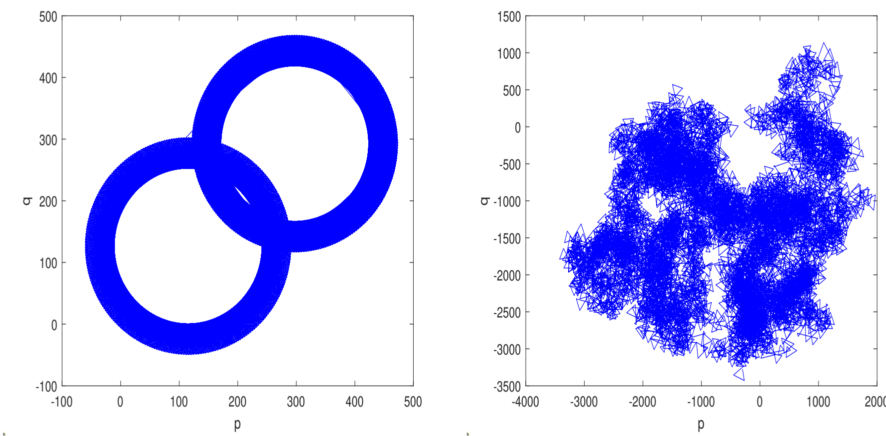

(a) (b)

FIGURE 5. The $0-1$ test for map (3.5) (APD vs t_s) with fixed memory length $F = 2800$, fractional order $v = 0.95$ and initial condition $APD_1 = 260msec$, for: (a) $t_s = 250msec$, (b) $t_s = 150msec$.

decrease of t_s the value of K is fixed at one.
These results are consistent and confirm what we previously concluded through the bifurcation diagram for the same parameters F, v and APD_1.

Physiologically, there is a link between chaos and Arrhythmogenesis, the regular APD behavior ($K \approx 0$) corresponds to stable cardiac rhythm with predictable electrical activity, the period-doubling (alternans) (moderate K) reflects a state where APD alternates between two values, known to be a precursor to dangerous arrhythmias such as ventricular fibrillation, while chaotic APD behavior ($K \approx 1$) confirms the onset of chaos, which in cardiac physiology corresponds to irregular and potentially lethal arrhythmias (e.g., fibrillation) and suggests loss of deterministic control in APD regulation, making it more difficult to predict and control cardiac responses to pacing.

5. CONCLUSION

In this paper, we investigate the effect of fixed memory length on a one-dimensional mapping model of cardiac action potential amplitude using Caputo's fractional difference definition. By analyzing bifurcation diagrams of the proposed model, we examine its dynamic behavior and demonstrate that incorporating fixed memory length leads to distinct dynamics compared to the Lewis and Guevara model, which does not account for memory effects [22]. We notice that for $APD_1 \geq 248msec$ ($APD_1 = 260msec$), after the appearance of the $2:2$ rhythm, the $5:5$ rhythm appears, followed by the $3:3$ rhythm, which is different from what appeared in the previous models.
As for $APD_1 \leq 248msec$ ($APD_1 = 200msec$), chaos suddenly appears at $t_s = 305.7msec$, which is earlier than the appearance of chaos in the previous models. In addition, the appearance of chaos in our model was not preceded by the $2:2$

alternating rhythm, but appeared after it, in addition to the appearance of the $3 : 3$ rhythm, followed by the $6 : 6$ rhythm, which is also different from what appeared in the previous models.
We also get in this model a new bistability, which does not exist in the previous models (the model without memory and the short memory model) such as:

- The Bistability $\{2 : 2 \leftrightarrow chaos\}$.
- The Bistability $\{5 : 5 \leftrightarrow 3 : 3\}$.
- The Bistability $\{3 : 3 \leftrightarrow 6 : 6\}$.

To verify the obtained result, the $0 - 1$ test is utilized.

Future research should focus on feedback control methods like delayed feedback, adaptive control, and external pacing to suppress chaos and stabilize cardiac rhythms. Additionally, studying the synchronization between the proposed fractional-order model and the Guevara [22] model can reveal the impact of memory on coupled cardiac dynamics. Applying synchronization techniques, such as phase and complete synchronization, will help determine conditions for coherent electrical activity.

Acknowledgement. The authors would like to thank the Editor and the anonymous referees for their suggestions.

References

1. Abdeljawad, T. (2011). On Riemann and Caputo fractional differences. Computers & Mathematics with Applications, 62(3), 1602-1611. https://doi.org/10.1016/j.camwa.2011.03.036
2. Almatrafi, M. B., & Berkal, M. (2024). Bifurcation analysis and chaos control for fractional predator-prey model with Gompertz growth of prey population. Modern Physics Letters B, 2550103. https://doi.org/10.1142/S0217984925501039
3. Almatrafi, M. B., & Berkal, M. (2025). Stability and bifurcation analysis of predator-prey model with Allee effect using conformable derivatives. Journal of Mathematics and Computer Science, 36(3), 299-316. https://dx.doi.org/10.22436/jmcs.036.03.05
4. Almatrafi, M. B., & Berkal, M. (2023). Bifurcation analysis and chaos control for prey-predator model with Allee effect. International Journal of Analysis and Applications, 21, 131-131. https://dx.doi.org/10.28924/2291-8639-21-2023-131
5. Baumol, W. J., & Benhabib, J. (1989). Chaos: significance, mechanism, and economic applications. Journal of economic perspectives, 3(1), 77-105. https://dx.doi.org/10.1257/jep.3.1.77
6. Berkal, M., & Almatrafi, M. B. (2023). Bifurcation and stability of two-dimensional activator-inhibitor model with fractional-order derivative. Fractal and Fractional, 7(5), 344. https://doi.org/10.3390/fractalfract7050344
7. Berkal, M., & Navarro, J. F. (2021). Qualitative behavior of a two-dimensional discrete-time prey-predator model. Computational and Mathematical Methods, 3(6), e1193.. https://doi.org/10.1002/cmm4.1193
8. Berkal, M., Navarro, J. F., Hamada, M. Y., & Semmar, B. (2025). Qualitative behavior for a discretized conformable fractional-order predator-prey model. Journal of Applied Mathematics and Computing, 1-23. https://doi.org/10.1007/s12190-025-02413-3
9. Bououden, R., & Abdelouahab, M. S. (2018). On Efficient Chaotic Optimization Algorithm Based on Partition of Data Set in Global Research Step. Nonlinear Dynamics and Systems Theory, 18(1), 42-52.

10. Bououden, R., & Abdelouahab, M. S. (2021). Chaotic Optimization Algorithm Based on the Modified Probability Density Function of Lozi Map. Boletim da Sociedade Paranaense de Matemática, 39, 9-22. https://doi.org/10.5269/bspm.41668
11. Bououden, R., & Abdelouahab, M.S. (2020). Chaos in new 2-d discrete mapping and its application in optimisation. Nonlinear Dynamics and Systems Theory. 20(2), 144-152.
12. Boudjedour, A., Batiha, I., Boucetta, S., Dalah, M., Zennir, K., & Ouannas, A. (2025). A finite difference method on uniform meshes for solving the time-space fractional advection-diffusion equation. Gulf Journal of Mathematics, 19(1), 156-168. https://doi.org/10.56947/gjom.v19i1.2524
13. Babrhou, Y., Fatima Cherkaoui, El Boukari, B., Hilal, K., & Kajouni, A. (2025). Analysis and optimal control of a fractional-order SEAIR epidemic model with two-strains. Gulf Journal of Mathematics, 19(1), 251-284. https://doi.org/10.56947/gjom.v19i1.2561
14. Chen, A., & Chen, Y. (2011). Existence of solutions to anti-periodic boundary value problem for nonlinear fractional differential equations with impulses. Advances in Difference Equations, 2011, 1-17. https://doi.org/10.1155/2011/915689
15. Cherubini, C., Filippi, S., Gizzi, A., & Ruiz-Baier, R. (2017). A note on stress-driven anisotropic diffusion and its role in active deformable media. Journal of Theoretical Biology, 430, 221-228. https://doi.org/10.1016/j.jtbi.2017.07.013
16. Elsadany, A. A., & Matouk, A. E. (2015). Dynamical behaviors of fractional-order Lotka-Volterra predator–prey model and its discretization. Journal of Applied Mathematics and Computing, 49, 269-283. https://doi.org/10.1007/s12190-014-0838-6
17. Gizzi, A., Loppini, A., Ruiz-Baier, R., Ippolito, A., Camassa, A., La Camera, A., Emmi, E.,Di Perna, L. , Garofalo, V., Cherubini, C., & Filippi, S. (2017). Nonlinear diffusion and thermo-electric coupling in a two-variable model of cardiac action potential. Chaos: An Interdisciplinary Journal of Nonlinear Science, 27(9). https://doi.org/10.1063/1.4999610
18. Glass, L., & Mackey, M. C. (1988). From clocks to chaos: The rhythms of life. Princeton University Press.
19. Gleick, J. (1987) Chaos: Making a New Science. Viking Penguin, New York.
20. Goldberger, A. L., & West, B. J. (1987). Fractals in physiology and medicine. The Yale journal of biology and medicine, 60(5), 421.
21. Gottwald, G. A., & Melbourne, I. (2004). A new test for chaos in deterministic systems. Proceedings of the Royal Society of London. Series A: Mathematical, Physical and Engineering Sciences, 460(2042), 603-611. https://doi.org/10.1098/rspa.2003.1183
22. Guevara, M. R., Glass, L., & Shrier, A. (1981). Phase locking, period-doubling bifurcations, and irregular dynamics in periodically stimulated cardiac cells. Science, 214(4527), 1350-1353. https://doi.org/10.1126/science.731369
23. Guel-Cortez, A. J., & Kim, E. J. (2020). A fractional-order model of the cardiac function. In Chaotic Modeling and Simulation International Conference (pp. 273-285). Cham: Springer International Publishing. https://doi.org/10.1007/978-3-030-70795-8_21
24. Karma, A. (1994). Electrical alternans and spiral wave breakup in cardiac tissue. Chaos: An Interdisciplinary Journal of Nonlinear Science, 4(3), 461-472. https://doi.org/10.1063/1.166024
25. Köme, C., & Yazlik, Y. (2024). Stability, bifurcation analysis and chaos control in a discrete predator-prey system incorporating prey immigration. Journal of Applied Mathematics and Computing, 70(5), 5213-5247. https://doi.org/10.1007/s12190-024-02230-0
26. Kumar, A., Bahuguna, D., & Kumar, S. (2024). Complex dynamic behaviour on fractional predator-prey model of mathematical ecology. Journal of Applied Mathematics and Computing, 70(6), 5319-5357. https://doi.org/10.1007/s12190-024-02171-8
27. Landaw, J., Garfinkel, A., Weiss, J. N., & Qu, Z. (2017). Memory-induced chaos in cardiac excitation. Physical review letters, 118(13), 138101. https://doi.org/10.1103/PhysRevLett.118.138101

28. Lewis, T. J., & Guevara, M. R. (1990). Chaotic dynamics in an ionic model of the propagated cardiac action potential. Journal of theoretical biology, 146(3), 407-432. https://doi.org/10.1016/S0022-5193(05)80750-7
29. Lorenz, E. N. (1963). Deterministic nonperiodic flow. Journal of the Atmospheric Sciences, 20(2), 130-141. https://doi.org/10.1175/1520-0469(1963)020<0130:DNF>2.0.CO;2
30. Magin, R.L. (2006) Fractional Calculus in Bioengineering. Begell House Publishers, Redding.
31. Miller, K. S., & Ross, B. (1989, May). Fractional difference calculus. In Proceedings of the international symposium on univalent functions, fractional calculus and their applications.
32. Nolasco, J. B., & Dahlen, R. W. (1968). A graphic method for the study of alternation in cardiac action potentials. Journal of applied physiology, 25(2), 191-196. https://doi.org/10.1152/jappl.1968.25.2.191
33. Otani, N. F. (2017). Theory of the development of alternans in the heart during controlled diastolic interval pacing. Chaos: An Interdisciplinary Journal of Nonlinear Science, 27(9). https://doi.org/10.1063/1.5003250
34. Otani, N. F., & Gilmour Jr, R. F. (1997). Memory models for the electrical properties of local cardiac systems. Journal of Theoretical Biology, 187(3), 409-436. https://doi.org/10.1006/jtbi.1997.0447
35. Peters, E. E. (1996). Chaos and order in the capital markets: a new view of cycles, prices, and market volatility. John Wiley & Sons.
36. Qu, Z., Weiss, J. N., & Garfinkel, A. (1999). Cardiac electrical restitution properties and stability of reentrant spiral waves: a simulation study. American Journal of Physiology-Heart and Circulatory Physiology, 276(1), H269-H283. https://doi.org/10.1152/ajpheart.1999.276.1.H269
37. Stenzinger, R. V., & Tragtenberg, M. H. R. (2022). Cardiac reentry modeled by spatiotemporal chaos in a coupled map lattice. The European Physical Journal Special Topics, 231(5), 847-858. https://doi.org/10.1140/epjs/s11734-022-00473-1
38. Strogatz, S. H. (2018). Nonlinear Dynamics and Chaos: With Applications to Physics, Biology, Chemistry, and Engineering. Westview Press. https://doi.org/10.1201/9780429492563
39. Sun, H., & Chang, Y. (2015). Fractional-order modeling of action potential duration restitution in cardiac tissue. Communications in Nonlinear Science and Numerical Simulation, 27(1-3), 1-11.
40. Wang, X., et al. (2024). Impact of Ionic Accumulation on APD Dynamics in Pathological Conditions. Journal of Cardiac Electrophysiology, 35(4), 567-578.
41. Weiss, J. N., Garfinkel, A., Karagueuzian, H. S., Chen, P. S., & Qu, Z. (2010). Early afterdepolarizations and cardiac arrhythmias. Heart rhythm, 7(12), 1891-1899. https://doi.org/10.1016/j.hrthm.2010.09.017
42. Weiss, J. N., Garfinkel, A., Karagueuzian, H. S., Chen, P. S., & Qu, Z. (2010). Early afterdepolarizations and cardiac arrhythmias. Heart rhythm, 7(12), 1891-1899. https://doi.org/10.1016/j.hrthm.2010.09.017
43. Zhao, Y., et al. (2022). Advancements in Space-Fractional Models for Cardiac Wave Propagation. Computational Biology, 29(3), 345-359.

[1] Laboratory of Mathematics and their Interactions, Department of Mathematics, Abdelhafid Boussouf University Center, Algeria.
Email address: a.bellout@centre-univ-mila.dz

[2] Department of Applied Mathematics, Abdelhafid Boussouf University Center, Mila ,R.P 26, Mila, 43000, Algeria.
Email address: r.bouden@centre-univ-mila.dz

[3] Laboratory of Applied Mathematics and Modeling, Department of Mathematics, Faculty of Exact Sciences, University of Constantine 1, Constantine, Algeria
Email address: tarek_houmor@umc.edu.dz

[4] Department of Mathematics, University of Alicante, 03690,, San Vicente del Raspeig, Alicante, Spain
Email address: berkalmessaoud@gmail.com